

## [EN-103] Development of Trajectory Prediction Model

<sup>+</sup>Yutaka Fukuda\*, Masayuki Shirakawa\*, Atsushi Senoguchi\*

\*Air Traffic Management Department  
Electronic Navigation Research Institute (ENRI)  
Tokyo, Japan  
[fukuda | shirakawa | senoguchi]@enri.go.jp

**Abstract:** This paper describes a trajectory prediction model and prediction accuracy error analysis for the climb and descent phases of flight. This model predicts trajectories based on aircraft performance, airline operation, the navigation database, and weather forecasts. In order to attain the required accuracy for operational use, uncertainty factor analysis based on actual flight operation environments is important. Predicted trajectories using the model are compared with recorded flight data. Error factors from the aircraft speed model and error factors from weather forecasts were analyzed for ground speed predictions. BADA (Base of Aircraft Data) from EUROCONTROL was used as the aircraft speed model. The numerical forecast model of the Japan Meteorological Agency (JMA) is used for weather forecasts. As a result, the speed difference between the aircraft speed model and actual operation were larger than the weather forecast error. The operational speed is smaller than the aircraft speed model in most samples. It is estimated that more fuel saving flights are selected in actual flight.

**Keywords:** Air Traffic Management, Trajectory Based Operation, Trajectory Prediction Model

### 1. INTRODUCTION

Trajectory Based Operation (TBO) is considered to be a key concept of Air Traffic Management (ATM) into the future. Trajectory is *a description of the movement of an aircraft, both in the air and on the ground, including position, time and, through calculation, speed and acceleration* [1]. A trajectory is generated based on the expectations of the flight operator in consideration of various elements, such as aircraft performance and weather conditions. It is modified to avoid hazards such as bad weather and conflict with other aircraft. All flight phases from departure to arrival can be uniformly managed by TBO, and in this way, flight operation efficiency can be improved.

NextGen (The Next Generation Air Transportation System) of the United States and SESAR (The Single European Sky ATM Research Program) of Europe aim to achieve TBO [2], [3]. CARATS (Collaborative Actions for Renovation of Air Traffic Systems) is being discussed in Japan [4]. TBO is one of the target concepts.

Aircraft have a Flight Management System (FMS), which generates the optimum trajectory for fuel consumption and flight time. Trajectory optimization is limited to individual aircraft. It does not work for all aircraft. Aircraft equipped with the latest FMS have highly accurate trajectory control. But old aircraft do not have this function. Therefore, a ground-based trajectory prediction and control system for all aircraft is required for TBO and overall aircraft optimization.

The Electronic Navigation Research Institute (ENRI) is developing a trajectory prediction model for TBO [5]-[9]. It generates precise four-dimensional trajectories (4DT) using aircraft performance data and weather forecast data, etc. ENRI compares trajectories generated from the prediction model with operational data, and carries out prediction error analysis.

This paper describes the trajectory prediction model and prediction error analysis on the climb and descent phases of flight. Firstly, the method of trajectory prediction is shown. Secondly, the paper analyzes the error factors that influence trajectory prediction accuracy. Trajectories predicted by the trajectory prediction model are compared with the trajectories of operational data. Error factors from weather forecasts and the aircraft speed model are analyzed.

### 2. METHOD OF TRAJECTORY PREDICTION

Figure 1 shows a block diagram of the trajectory prediction model. It uses aircraft performance data, the airline operation model, a navigation database, and weather forecast data, etc. A Total Energy Model (TEM) is used as the aircraft model [10]. The TEM equates the rate of work done by forces acting on the aircraft to the rate of increase in potential and kinetic energy.

The aircraft performance data includes the flight envelope of each aircraft model (maximum speed, minimum speed, etc.), aerodynamics (wing area and drag coefficient), engine thrust, fuel consumption, etc. The airline operation model includes standard altitude, speed, and weight during the climb, cruise, and

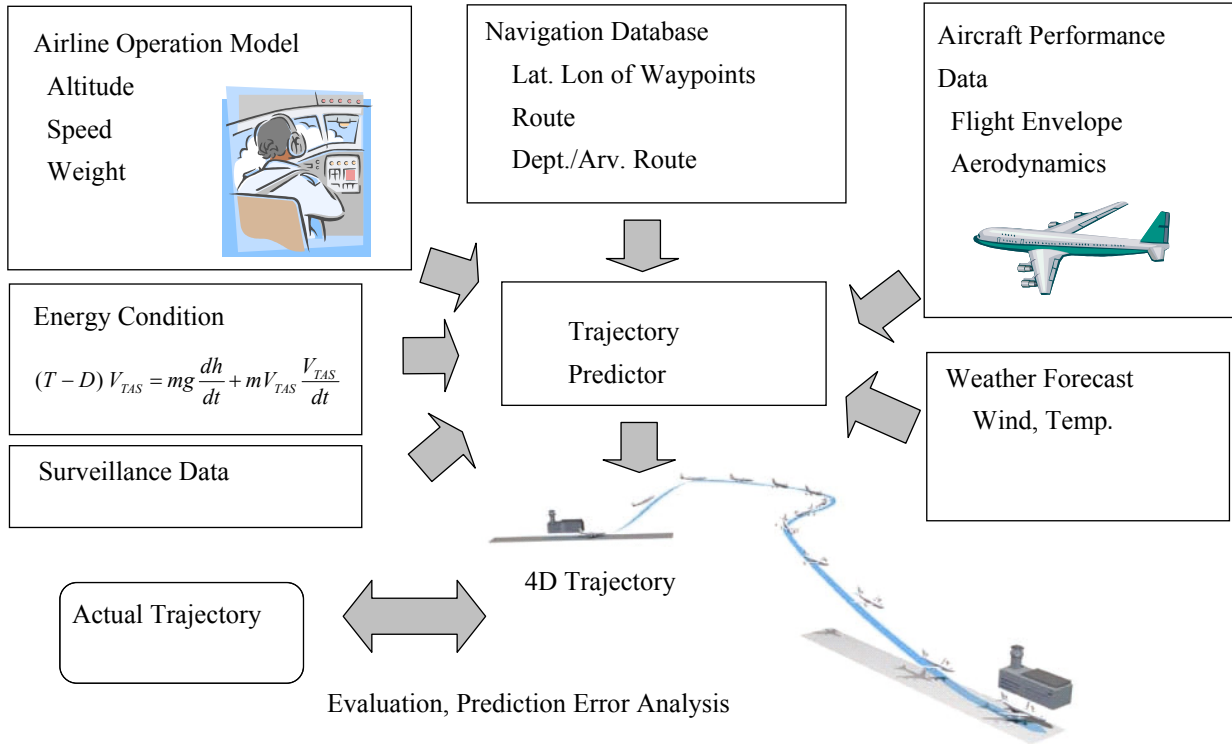


Figure 1. Block Diagram of Trajectory Prediction Model

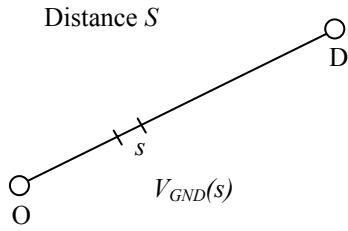


Figure 2. Flight Time Prediction

descend phases. BADA (Base of Aircraft Data) by EUROCONTROL is used for this data. The navigation database provides positional data for routes and waypoints. ARINC424 data is used as a navigation database [11]. Surveillance data includes an aircraft’s current position and speed. It is used to monitor and update trajectories.

In order to calculate the flight time to a waypoint from the present position, Ground Speed (GS) and distance along the route are used. The total flight time is calculated as the sum of small segment flight times. Total flight time  $T_p$  from origin O to destination D in Figure 2 is given by Eq. (1).

$$T_p = \int_0^S \frac{1}{V_{GND}(s)} ds \quad (1)$$

where  $S$  is the distance from origin O to destination D,  $s$  is small segment distance, and  $V_{GND}(s)$  is GS at the small segment. The distance can be calculated accurately by using the RNAV (Area Navigation) route [12]. The accuracy of GS predictions is important. The

size of the small segment is decided with an aircraft’s wind-influenced changes in GS.

The aircraft usually flies at a constant Indicated Air Speed (IAS) or Calibrated Air Speed (CAS) and Mach number. The trajectory prediction model converts the CAS or Mach number into True Air Speed (TAS). GS is calculated, taking into account the influence of wind aloft.

Eq. (2) shows the relationship between TAS  $V_{TAS}$  and CAS  $V_{CAS}$  [10].

$$V_{TAS} = \left[ \frac{2P}{\mu P} \left\{ 1 + \frac{(P_0)_{ISA}}{P} \left[ \left( 1 + \frac{\mu (\rho_0)_{ISA}}{2 (P_0)_{ISA}} V_{CAS}^2 \right)^{\gamma/\mu} - 1 \right]^\mu - 1 \right\} \right]^{1/2} \quad (2)$$

where  $P$  is the pressure at altitude,  $\rho$  is the air density at altitude,  $\gamma$  is the isentropic expansion coefficient for air = 1.4, and  $\mu = (\gamma - 1)/\gamma$ . ISA stands for International Standard Atmosphere,  $(P_0)_{ISA}$  is the ISA pressure at sea level = 101325 Pa, and  $(\rho_0)_{ISA}$  is the ISA air density at sea level = 1.225 kg/m<sup>3</sup>. Air pressure  $P$  and density  $\rho$  are given as functions of temperature.

$$P = (P_0)_{ISA} \left[ T/T_0 \right]^{-\frac{g}{k_T R}} \quad (3)$$

$$\rho = \rho_0 \left[ T/T_0 \right]^{\frac{g}{k_T R} - 1} \quad (4)$$

where  $T$  is the temperature at altitude (K),  $T_0$  is the temperature at sea level,  $\rho_0$  is the air density at sea

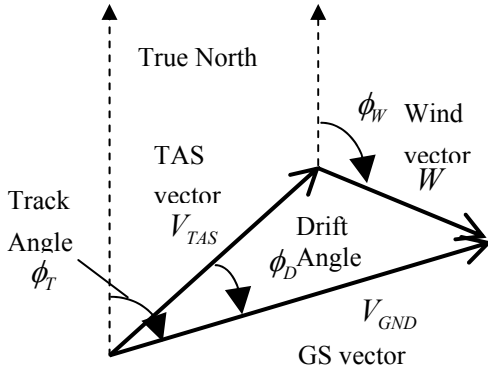


Figure 3. GS Calculation

level,  $R$  is the real gas constant for air,  $g$  is gravity acceleration,  $K_T$  is the ISA temperature gradient with altitude,  $-g/K_T R = 5.25583$ .

Eq. (5) shows the relationship between TAS  $V_{TAS}$  and Mach number  $M$ .

$$V_{TAS} = M\sqrt{\gamma \cdot R \cdot T} \quad (5)$$

The transition altitude is the boundary between CAS-based operation and Mach-based operation. When the altitude is above the transition altitude, the Mach number is used to calculate TAS. On the other hand, when the altitude is below the transition altitude, CAS is used.

The GS is calculated by TAS and the wind vector (Figure 3). GS is calculated by Eq. (6) [7].

$$V_{GND} = V_{TAS} \cos \phi_D + W \cos(\phi_W - \phi_T) \quad (6)$$

where  $W$  is Wind Speed (WS),  $\phi_W$  is Wind Direction (WD),  $\phi_T$  is track angle, and  $\phi_D$  is drift angle.  $\phi_D$  is calculated by Eq. (7).

$$\phi_D = \sin^{-1} \left( \frac{W}{V_{TAS}} \sin(\phi_W - \phi_T) \right) \quad (7)$$

TEM is used for movement calculation in the climb and descend phases.

$$(T - D)V_{TAS} = mg \frac{dh}{dt} + mV_{TAS} \frac{dV_{TAS}}{dt} \quad (8)$$

where  $T$  is thrust,  $D$  is drag,  $m$  is aircraft mass,  $h$  is altitude, and  $t$  is time. The rate of work done by forces (thrust and drag) acting on the aircraft equals the rate of increase in potential and kinetic energy. Potential energy corresponds to altitude, and kinetic energy corresponds to TAS. For example, the descent rate at constant CAS and idle thrust is calculated by solving Eq. (2) and (8) with parameters for thrust, drag, and CAS.

WD, WS, and temperature are calculated using weather forecasts from the Japan Meteorological

Agency (JMA). They are defined at a three-dimensional grid point (latitude, longitude, and altitude) in the atmosphere. A numerical forecast model of the Global Scale Model (GSM) or the Meso Scale Model (MSM) are used. The grid point data is interpolated into continuous four-dimensional data, using latitude, longitude, altitude and time.

### 3. COMPARISON OF PREDICTION AND MEASUREMENT

#### 3.1 Comparison of climb phase

Figure 4 through Figure 8 show an example of climb trajectory comparison. The horizontal axis is the flight time. The predicted speed of a medium type aircraft is compared with its measured speed. For the calculation of prediction data, reduced climb thrust is used. This is from 85 % to 100 % of standard climb thrust for fuel saving, depending on the aircraft's weight. The CAS or Mach number is obtained from the speed of the BADA airline operation model. It is converted into TAS using forecast temperature. GS is calculated by adding the forecast wind. The weather forecast data is interpolated from the MSM delivered before the aircraft departure time. The actual altitude and weight is used in calculating the prediction. The measured speed is recorded by the aircraft. Though the precision of the measurements are not known, it is assumed to be true because it is measured and calculated by the aircraft.

Figure 4 shows the measured altitude profile of the aircraft. Figure 5 compares measured and predicted CAS. Predicted CAS is based on the BADA airline operation model. Predicted CAS changes instantaneously at 4,000 ft, 5,000 ft, 6,000 ft, and 10,000 ft (1 ft = 0.3048 m). Measured CAS changes from 250 kt to 290 kt in 42 s transition time (1 kt = 0.514 m/s). Acceleration rate is about 0.95 kt/s. CAS is restricted to less than 250 kt below 10,000ft by Air Traffic Control (ATC) procedures. There is a 10 kt CAS difference between the predicted CAS of 300 kt and the measured CAS of 290 kt above 10,000 ft. Aircraft cross the CAS and Mach transition altitude at 11:48. The CAS decreases with constant Mach operation above transition altitude.

Figure 6 compares measured and predicted GS. TAS and GS increase while the aircraft climbs with constant CAS. This is why air density decreases from low altitude to high altitude. Predicted GS corresponds well to measured GS.

Figure 7 compares measured and predicted WS along an aircraft's trajectory. Measured WS changes up and down more than predicted WS. The predicted WS is in the mid range of the measured WS. The difference between measured WS and predicted WS is less than 10 kt.

Figure 8 shows the error factor of GS from WS, WD, temperature, and CAS. This data is calculated from a

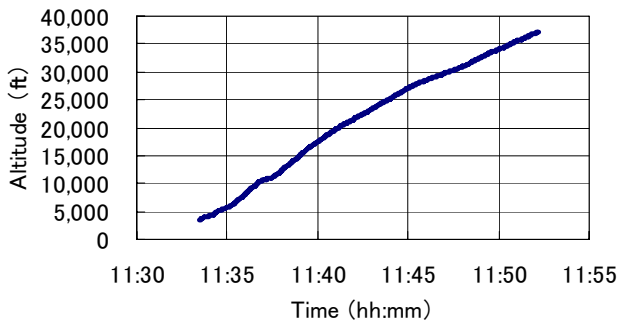


Figure 4 Altitude (CLB)

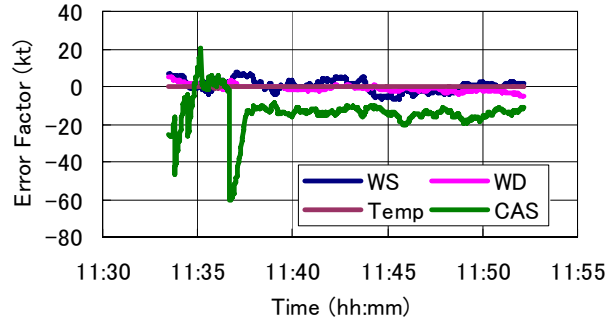


Figure 8 Error Factor (CLB)

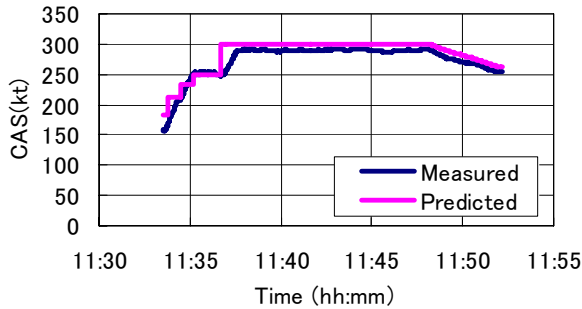


Figure 5 CAS (CLB)

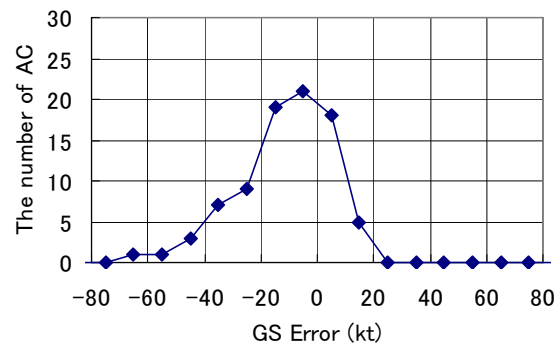


Figure 9 GS Error Distribution (CLB)

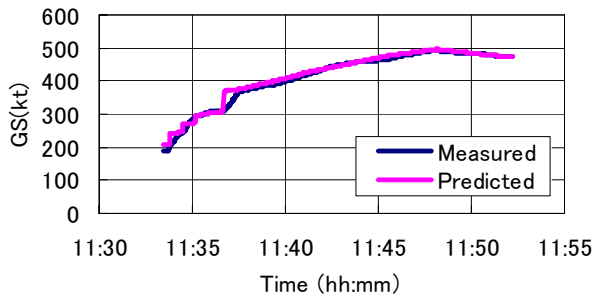


Figure 6 GS (CLB)

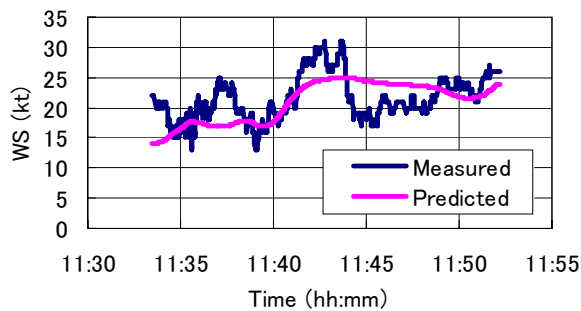


Figure 7 WS (CLB)

partial derivative of Eq. (6) [7], [8]. This represents the degree of influence of each factor on GS error. Air temperature and WD are small. WS is less than 10 kt. CAS is about -15 kt after 11:38. This means that the measured CAS is smaller than the predicted CAS. The CAS error factor is larger than the wind forecast error factor. The average GS error in the climb phase is -5.34 kt in this sample.

Figure 9 shows a histogram of average GS error. The number of aircraft in the sample is 84. The histogram of GS error shifts to a negative value. This means that

the measured GS is smaller than the predicted GS. It is estimated that more fuel saving flight is selected in actual operation, because slower GS saves fuel consumption.

### 3.2 Comparison of descent phase

Figure 10 to Figure 14 show an example of descent trajectory comparison for the same aircraft. The speed calculation is the same as for the climb. The thrust is nominal descent thrust. It is almost the same as idle thrust.

Figure 10 shows the measured altitude profile of the aircraft. Figure 11 compares measured and predicted CAS. Predicted CAS changes instantaneously at 10,000 ft, 6,000 ft, 3,000 ft, 2,000 ft and 1,500 ft. Measured CAS reduces gradually earlier than predicted CAS mostly. Measured CAS reduces from 290 kt to 250 kt about 1 min. Deceleration rate is 0.64 kt/s. In CAS transition period, CAS error is large. There are 10 kt CAS difference between predicted CAS of 290 kt and measured CAS of 280 kt above 20,000 ft.

Figure 12 compares measured and predicted GS. TAS and GS decrease while the aircraft descends with constant CAS. Measured and predicted GS are almost the same. CAS differences at CAS transition periods affect GS differences. The predicted GS corresponds well to the measured GS.

Figure 13 compares the measured and predicted WS along the aircraft's trajectory. Measured WS changes up and down more than predicted WS. The predicted WS is in the mid range of the measured WS. The

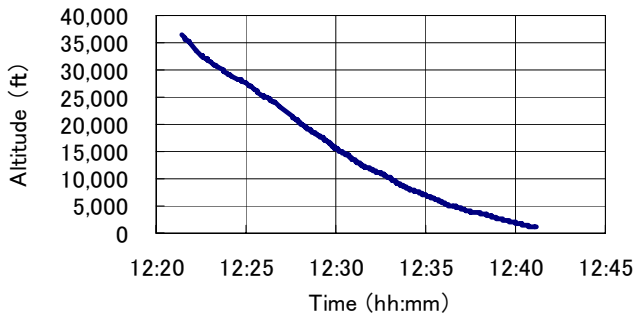


Figure 10 Altitude (DES)

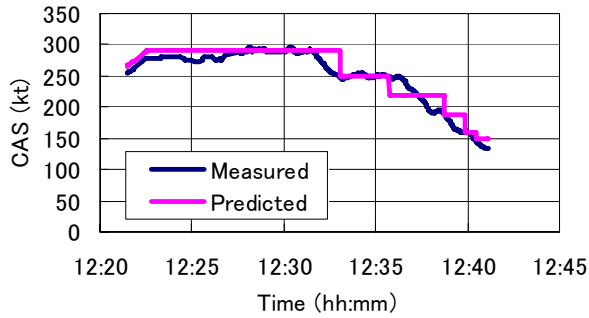


Figure 11 CAS (DES)

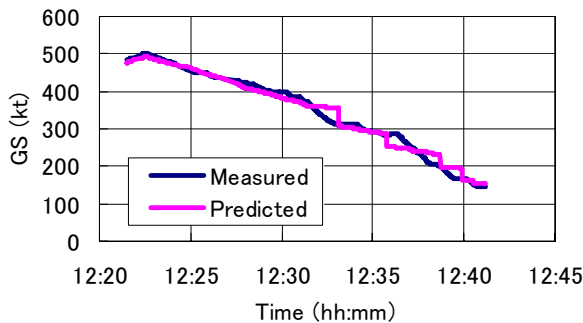


Figure 12 GS (DES)

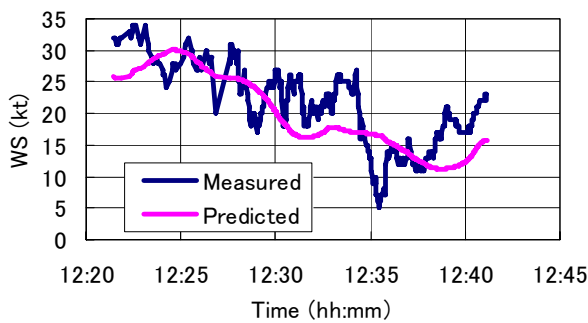


Figure 13 WS (DES)

difference between the measured and predicted WS is less than 10 kt.

Figure 14 shows the error factor for GS from WS, WD, temperature, and CAS. Air temperature and WD are small. WS is less than 10 kt. of the CAS factor is large at CAS transition periods and at high altitude. The CAS error factor is larger than the weather error factor. The average GS error in the descent phase is +0.44 kt in this sample.

Figure 15 shows a histogram of average GS error. The number of aircraft in the sample is 85. The histogram

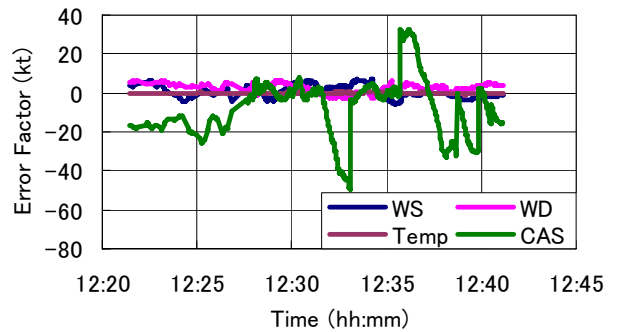


Figure 14 Error Factor (DES)

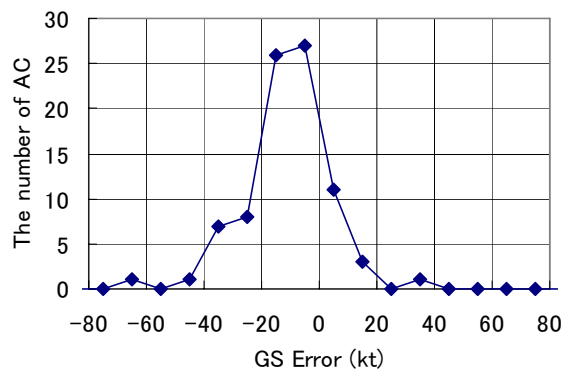


Figure 15 GS Error Distribution (DES)

of GS error shifts to a negative value. This means that the measured GS is smaller than the predicted GS. It is estimated that speed reduction is assigned by ATC for sequencing and spacing to the destination airport and more fuel saving flight is selected in actual operation.

The aircraft speed setting is decided in consideration of various conditions, such as aircraft weight, fuel costs, weather conditions, and delays. The speed is influenced by the cost index (CI) of FMS [13]. In the analysis, the measured GS was smaller than the predicted GS in many samples.

ICAO recommend that speed changes in the cruise phase of more than 5 % of TAS from their given flight plan shall be reported to an air traffic services unit [14]. In the future, it will be useful to acquire the intended speed of all flight phases for trajectory prediction with SWIM (System Wide Information Management). The Mach number and CAS information can be acquired by data communication with the DAPs (Downlink Aircraft Parameters) function of SSR (Secondary Surveillance Radar) mode S and ADS-B (Automatic Dependent Surveillance-Broadcast). It is useful to take into account such surveillance information for trajectory prediction.

With regard to weather forecasts, monitoring current wind and temperature is important. Currently, some aircraft have a wind information downlink function. If forecast errors compared with the aircraft's monitored weather data increase in some areas, trajectory prediction accuracy decreases in the areas. In this case, measures are taken such as weather forecast update

delivery or error margin expansion for trajectory prediction.

#### 4. SUMMARY

This paper has provided a trajectory prediction model and prediction accuracy error analysis on the climb and descent phases of flight. Trajectories predicted by the trajectory prediction model are compared with the trajectories of operational data.

Error factors due to the aircraft speed model and error factors due to weather forecasts were analyzed for GS prediction. As a result, the Mach number and CAS difference between the airline operation model and measurement data were large in most cases where the GS difference was large. Airline operation model error was larger than weather forecast error. The measured CAS is smaller than that of the airline operation model in most cases. It is estimated that more fuel saving flight is selected in actual operation.

Detailed analysis is being considered for future study when weather forecast error is large. Climb and descent rate analysis is required to define the position uncertainty of 4DT. The development of algorithms to modify trajectories in order to resolve conflicts and to adjust speed for CTA (Controlled Time of Arrival) is for future study.

#### ACKNOWLEDGMENTS

The authors would like to express thanks to all parties who cooperated in this research.

#### REFERENCES

- [1] ICAO, "Global Air Traffic Management Operational Concept", ICAO Doc 9854AN/458, 2005
- [2] Joint Planning and Development Office. "Concept of Operation for the Next Generation Air Transportation System Ver.3.1", April 2010
- [3] SESAR Joint Undertaking, "European Air Traffic Management Master Plan. Edition 1". March 2009
- [4] Working Group on Future Air Traffic System. CARATS (Collaborative Actions for Research of Air Traffic Systems). 2010
- [5] Shirakawa M, Fukuda Y and Senoguchi A. "Trajectory predictions with the aircraft performance models". IEICE Technical Report SANE 2008-99, Jan. 2009.
- [6] Fukuda Y, Shirakawa M and Senoguchi A. "Study on Trajectory Prediction Models". ENRI International Workshop on ATM/CNS (EIWAC) 2009, March 2009.
- [7] Shirakawa M, Fukuda Y and Senoguchi A. "Aircraft Trajectory Prediction Error Analysis". IEICE Technical Report SANE 2009-167, Feb. 2010.
- [8] Fukuda Y, Shirakawa M and Senoguchi A. "Development and Evaluation of Trajectory Prediction Model". 27th International Congress of the Aeronautical Sciences, Sept. 2010.
- [9] Shirakawa M, Fukuda Y and Senoguchi A. "A Study on Aircraft Vertical Trajectories". 48th Aircraft Symposium, Dec. 2010.
- [10] Eurocontrol Experimental Center. "User Manual for the Base of Aircraft Data (BADA), revision 3.7". EEC Technical/Scientific Report No.2008-0003, March 2009.
- [11] "Navigation Systems Data Base", ARINC Specification 424-18, 2005.
- [12] Fukuda Y, Shirakawa M. "Analysis of RNAV Departures and Arrivals Using Track Data". APISAT-2009, Nov. 2009
- [13] Rumler W, Gunther T, Fricke H, Weißhaar U, "Flight Profile Variations due to the Spreading Practice of Cost Index Based Flight Planning", ICRA-2010, June 2010.
- [14] "International Standards Annex 2, Rules of the Air Tenth Edition", ICAO, July 2005.

#### COPYRIGHT

##### Copyright Statement

The authors confirm that they, and/or their company or institution, hold the copyright of all original material included in this paper. They also confirm they have obtained permission, from the copyright holder of any third party material included in their paper, to publish it as part of their paper. The authors grant full permission for the publication and distribution of their paper as part of the EIWAC 2010 proceedings or as individual prints from the proceedings.